Theory comparison and numerical benchmarking on neoclassical toroidal viscosity torque

Zhirui Wang, Jong-Kyu Park, Yueqiang Liu, Nikolas Logan, Kimin Kim, and Jonathan E. Menard

---

Articles you may be interested in

Evaluation of the toroidal torque driven by external non-resonant non-axisymmetric magnetic field perturbations in a tokamak
Phys. Plasmas 21, 092506 (2014); 10.1063/1.4894479

Measurements of the deuterium ion toroidal rotation in the DIII-D tokamak and comparison to neoclassical theorya)
Phys. Plasmas 19, 056107 (2012); 10.1063/1.3694656

Entropy production rate in tokamaks with nonaxisymmetric magnetic fields
Phys. Plasmas 17, 072505 (2010); 10.1063/1.3454365

Nonlinear simulation of toroidal Alfvén eigenmode with source and sink
Phys. Plasmas 17, 042309 (2010); 10.1063/1.3394702

Collisionality dependence of the polarization current caused by a rotating magnetic island
Phys. Plasmas 12, 072501 (2005); 10.1063/1.1937338

Theory comparison and numerical benchmarking on neoclassical toroidal viscosity torque

Zhirui Wang,[1] Jong-Kyu Park,[1] Yueqiang Liu,[2] Nikolas Logan,[1] Kimin Kim,[1] and Jonathan E. Menard[1]

[1]*Princeton Plasma Physics Laboratory, Princeton, New Jersey 08543, USA*
[2]*Euratom/CCFE Association, Culham Science Centre, Abingdon OX14 3DB, United Kingdom*

Systematic comparison and numerical benchmarking have been successfully carried out among three different approaches of neoclassical toroidal viscosity (NTV) theory and the corresponding codes: IPEC-PENT is developed based on the combined NTV theory but without geometric simplifications [Park *et al.*, Phys. Rev. Lett. **102**, 065002 (2009)]; MARS-Q includes smoothly connected NTV formula [Shaing *et al.*, Nucl. Fusion **50**, 025022 (2010)] based on Shaing's analytic formulation in various collisionality regimes; MARS-K, originally computing the drift kinetic energy, is upgraded to compute the NTV torque based on the equivalence between drift kinetic energy and NTV torque [J.-K. Park, Phys. Plasma **18**, 110702 (2011)]. The derivation and numerical results both indicate that the imaginary part of drift kinetic energy computed by MARS-K is equivalent to the NTV torque in IPEC-PENT. In the benchmark of precession resonance between MARS-Q and MARS-K/IPEC-PENT, the agreement and correlation between the connected NTV formula and the combined NTV theory in different collisionality regimes are shown for the first time. Additionally, both IPEC-PENT and MARS-K indicate the importance of the bounce harmonic resonance which can greatly enhance the NTV torque when $\mathbf{E} \times \mathbf{B}$ drift frequency reaches the bounce resonance condition. © 2014 AIP Publishing LLC. [http://dx.doi.org/10.1063/1.4869251]

I. INTRODUCTION

It is known that the toroidal asymmetry produced by non-axisymmetric magnetic perturbations in tokamaks can cause a substantial damping of toroidal flow through the neoclassical toroidal viscosity (NTV) torque. Therefore, the NTV torque can provide a promising way to externally optimize plasma rotation and rotation shear, thereby improving plasma instabilities and performance, as has been highlighted by recent experiments.[1–5] In order to increase the predictability for NTV and the controllability for plasma rotation in tokamaks, it is important to understand the different approaches of NTV theory with proper cross-benchmark.

To study the NTV physics, various semi-analytic methods have been developed in recent years. In general, the methods find the NTV torque by solving the bounce averaged drift kinetic equation with approximations which depend on the approaches. There are mainly three different approaches with corresponding codes established. In the first approach, following the combined NTV theory[6] but without the geometric simplification, the IPEC-PENT code[7] is developed to perform the NTV computation with an effective Krook collisional operator, where the torque caused by the resonance with the precession motion ($l = 0$) and the particle bounce motion ($l \neq 0$) of trapped particles are considered. Here, l denotes the Fourier harmonic number of bounce motion. The effects due to different particle motions are combined by a generalized equation. The second approach, extensively developed by Shaing,[8] focuses on the precession motion of trapped particles. A simple connection formula is used to smoothly connect the formulations in different collisionality regimes—the so called smoothly connected NTV

formula. The analytic formulation with an appropriate simplification of toroidal geometry has been derived by considering the separation of collisionality regimes. Particularly, in this approach, the full pitch angle scattering collisional operator is included, which can be more accurate and important in the low collisionality regime. This semi-analytic approach has been implemented in MARS-Q.[9,10] The third approach is based on the equivalence between the drift kinetic energy and the NTV torque due to trapped particles as shown in Ref. 11. Similar to the NTV torque caused by magnetic perturbations, the drift kinetic theory in the study of the ideal MHD stability of modes, such as the resistive wall mode (RWM),[12–19] takes into account the mode-particle interaction derived from the perturbed drift kinetic equation. The MARS-K code,[20] which has been applied to the RWM studies, is upgraded to compute the NTV torque following this approach. The NTV torque due to precession and bounce resonances of trapped particles are included in the code.

In the present work, a systematic verification of these three different semi-analytic NTV approaches, as well as a numerical benchmarking among IPEC-PENT and MARS-K/Q, is carried out. This paper is organized as follows. Section II describes the model of ideal perturbed equilibrium and the neoclassical toroidal viscosity models in IPEC-PENT and MARS-K/Q. The equivalence between the combined NTV torque and drift kinetic energy in MARS-K is demonstrated. Section III reports the benchmark results of perturbed equilibrium, as well as the NTV torques computed by IPEC-PENT, MARS-K/Q with respect to the three different approaches. The NTV torques due to the precession resonance ($l = 0$) and bounce resonance ($l \neq 0$) of trapped ions are investigated. Section IV summarizes the work.

II. MODELS AND FORMULATIONS

A. Ideal perturbed equilibrium model

The IPEC-PENT code solves the ideal perturbed equilibrium (1) based on the perturbed force balance[21] in toroidal system. The force balance equation is linearized in the presence of the external perturbed field

$$\vec{j} \times \vec{B} + \vec{J} \times \vec{b} - \nabla p = 0, \tag{1a}$$

$$p = -\vec{\xi} \cdot \nabla P - \Gamma P \nabla \cdot \vec{\xi}, \tag{1b}$$

$$\vec{b} = \nabla \times (\vec{\xi} \times \vec{B}), \tag{1c}$$

$$\vec{j} = \nabla \times \vec{b}. \tag{1d}$$

The perturbed quantities $\vec{\xi}, \vec{b}, \vec{j},$ and p denote the plasma displacement, magnetic field, current, and pressure, respectively. $\vec{B}, \vec{J}, P,$ and ρ represent the equilibrium variables of magnetic field, current, fluid pressure, and plasma density on the unperturbed flux surface. $\Gamma = 5/3$ is the ratio of specific heats.

Since the perturbed equilibrium is a linear problem and unperturbed equilibria are axisymmetric in tokamaks, the toroidal harmonic numbers n are decoupled and can be treated separately. Therefore, only a single toroidal mode number n needs to be considered at one time. The external perturbation is assumed to have an $\exp(in\phi)$ dependence along the toroidal angle ϕ in both IPEC-PENT and MARS-K/Q.

MARS-K and MARS-Q are the two versions of MARS code with different modules dedicated to the computation of drift kinetic energy and NTV torque, respectively, therefore, the fluid part of MARS-K/Q solves the same linearized MHD equations in the toroidal geometry

$$\left(\frac{\partial}{\partial t} + in\Omega\right)\vec{\xi} = \vec{v} + (\vec{\xi} \cdot \nabla\Omega)R^2\nabla\phi, \tag{2a}$$

$$\rho\left(\frac{\partial}{\partial t} + in\Omega\right)\vec{v} = -\nabla p + \vec{j} \times \vec{B} + \vec{J} \times \vec{b}$$
$$- \rho[2\Omega\vec{Z} \times \vec{v} + (\vec{v} \cdot \nabla\Omega)R\hat{\phi}]$$
$$- \nabla \cdot (\rho\vec{\xi})\Omega\vec{Z} \times \vec{V}_0, \tag{2b}$$

$$\left(\frac{\partial}{\partial t} + in\Omega\right)\vec{b} = \nabla \times (\vec{v} \times \vec{B}) + (\vec{b} \cdot \nabla\Omega)R\hat{\phi} - \nabla \times (\eta\vec{j}), \tag{2c}$$

$$\left(\frac{\partial}{\partial t} + in\Omega\right)p = -\vec{v} \cdot \nabla P - \Gamma P\nabla \cdot \vec{v}, \tag{2d}$$

$$\vec{j} = \nabla \times \vec{b}, \tag{2e}$$

where $\vec{v}$ is the perturbed velocity of the plasma, R is the plasma major radius, $\hat{\phi}$ is the unit vector along the geometric toroidal angle ϕ of the torus, and $\vec{Z}$ is the unit vector in the vertical direction in the poloidal plane. $\vec{V}_0$ is the plasma equilibrium flow $\vec{V}_0 = R\Omega\hat{\phi}$, with Ω being the angular frequency of the toroidal rotation. A conventional unit system is assumed with the vacuum permeability

$\mu_0 = 1$. On the right hand side of Eq. (2b), the fourth and fifth terms represent the Coriolis force and the centrifugal force, respectively.

For the purpose of plasma response modeling to the external perturbation in MARS-K/Q, the vacuum field equations outside the plasma, the thin resistive wall equation (when applicable), and the coil equations[22] are solved together with the MHD equations for the plasma in MARS-K/Q.

It is noted that when $\partial/\partial t \to 0$ and ignoring the plasma flow, inertia, and resistivity, MARS-K/Q can physically recover Eq. (1) to solve the perturbed equilibrium.

To compare the perturbed equilibrium computed by IPEC-PENT and MARS-K/Q, the external magnetic perturbation is generated by a source current $\vec{j}_{coil}$ flowing in the coil located in the vacuum region satisfying

$$\nabla \times \vec{b} = \vec{j}_{coil}, \quad \nabla \cdot \vec{j}_{coil} = 0.$$

B. NTV models

1. Combined NTV model in IPEC-PENT

IPEC-PENT computes the NTV torque derived from the volume integral of the general relation

$$T_\phi = \int dx^3 \left(\frac{\partial \vec{x}_L}{\partial \phi} \cdot \nabla \cdot \overset{\leftrightarrow}{\Pi}\right), \tag{3}$$

where $\vec{x}_L$ is the Lagrangian displacement, $\overset{\leftrightarrow}{\Pi} = p_\perp \overset{\leftrightarrow}{I} + (p_\parallel - p_\perp)\vec{b}\vec{b}$ is the anisotropic perturbed pressure tensor, $\vec{b} = \vec{B}/B$ is the unit vector of the equilibrium magnetic field, and B is the strength of the equilibrium field. The parallel and perpendicular components of the kinetic pressure $p_\parallel$ and $p_\perp$ are defined by

$$p_\parallel = \sum_{\alpha=e,i} \int d\Gamma M_\alpha v_\parallel^2 f_L^1, \tag{4}$$

$$p_\perp = \sum_{\alpha=e,i} \int d\Gamma \frac{1}{2} M_\alpha v_\perp^2 f_L^1. \tag{5}$$

The summation in Eqs. (4) and (5) is over the electron and ion components. The integral is carried out over the velocity space of trapped particles, where

$$d\Gamma = \frac{2\pi}{M_\alpha^2} \sum_\sigma d\varepsilon_k d\mu \frac{B}{|v_\parallel|}. \tag{6}$$

Here, M_α is the particle mass of ions or electrons, $v_\parallel$ and $v_\perp$ are the parallel and perpendicular velocity components of the particle, and $\sigma = \text{sign}(v_\parallel)$. The perturbed particle distribution function f_L^1 is derived by solving the bounce averaged perturbed drift kinetic equation[11] for each particle species. The neoclassical toroidal torque in terms of the kinetic pressure can be written as

$$T_\phi = -\int dx^3 \left[(p_\parallel - p_\perp)\frac{1}{B}\frac{\partial \delta B_L}{\partial \phi} + p_\parallel \frac{\partial}{\partial \phi}(\nabla \cdot \vec{\xi})\right], \tag{7}$$

where $\delta B_L = Q_{L\parallel} + \nabla B \cdot \vec{\xi}_\perp$ as the Lagrangian quantity is the variation of the field strength measured on the perturbed field lines, $Q_{L\parallel} = \vec{b} \cdot \nabla \times (\vec{\xi}_\perp \times \vec{B})$ is the magnetic perturbation in parallel direction of the equilibrium magnetic field, and $\vec{\xi}_\perp$ is the plasma displacement perpendicular to the equilibrium field line. Following the derivation in Ref. 11, the neoclassical toroidal torque of IPEC-PENT in the approximation of zero banana orbit width can be further written as

$$T_\phi = -n^2 \sum_{\alpha=e,i} \frac{1}{ZeM_\alpha^2} \int d\psi_p d\phi \int d\varepsilon_k d\mu \sum_l \mathcal{R}_l |\delta J_l|^2 \frac{\partial f_0}{\partial \psi_p}, \quad (8)$$

where f_0 is the Maxwellian equilibrium distribution function of thermal particles. $\varepsilon_k = \varepsilon - Ze\Phi$, where ε is the particle's total energy, ε_k is the kinetic energy of the particle, Φ is the equilibrium electrostatic potential, and Ze is the species charge (positive for ions and negative for electrons). The bounce-average action for the l-class of trapped particles is

$$\delta J_l = \tau_b \left\langle \left[(2\varepsilon_k - 3\mu B)\frac{\delta B_L}{B} + 2(\varepsilon_k - \mu B)\nabla \cdot \vec{\xi}_\perp \right] \mathcal{P}_l \right\rangle, \quad (9)$$

with an appropriate phase factor of trapped particles $\mathcal{P}_l = e^{-il\omega_b t}$.[11] l is the number of bounce harmonics. The resonant operator of trapped particles is defined as

$$\mathcal{R}_l = \frac{\omega_b \nu_{Dl} \hat{\varepsilon}_k^{-3/2}}{\left[l\omega_b - n(\omega_E + \omega_d) \right]^2 + \nu_{Dl}^2 \hat{\varepsilon}_k^{-3}}, \quad (10)$$

where ω_d is the magnetic precession frequency of trapped particles (ions or electrons) averaged over the bounce orbit, and ω_b is the bounce frequency of trapped particles. $\nu_{Dl} = \nu_\alpha/(2\epsilon)[1 + (l/2)^2]$, with $\alpha = i,e$ defined in Refs. 6 and 11 is the effective ion and electron collision frequency, $\nu_i = \nu_{ii}$ and $\nu_e \sim \nu_{ei}, \nu_{ee}$. ν_{ii}, ν_{ei}, and ν_{ee} are ion-ion, electron-ion, and electron-electron collision frequencies respectively in Ref. 23. $\epsilon \approx r/R$, where r is the minor radius. ω_E is the $\mathbf{E} \times \mathbf{B}$ drift due to the equilibrium electrostatic potential. $\hat{\varepsilon}_k = \varepsilon_k/T$ is the particle kinetic energy normalized by the temperature T. When $l = 0$, the precession motion of trapped particles can resonate with plasma $\mathbf{E} \times \mathbf{B}$ flow, $\omega_d \sim \omega_E$, the so-called precession resonance. As for $l \neq 0$, the bounce resonance can occur when $n\omega_E$ is comparable with $l\omega_b$.

2. The equivalence between kinetic energy in MARS-K and NTV in IPEC-PENT

MARS-K computes the drift kinetic energy δW_k through the kinetic pressure, $p_\parallel$ and $p_\perp$. In MARS-K, f_L^1 in Eqs. (4) and (5) is derived by solving the perturbed drift kinetic equation following approaches by Porcelli.[24] Though Porcelli's approach allows MARS-K to include the finite banana orbit width effects, they are neglected here for benchmarking with IPEC-PENT. Particularly, in the derivation of f_L^1 in Ref. 24, it is important to note that the second term in Eq. (22) from Ref. 24 is responsible for the radial drift of trapped particle banana orbits in a 3D field. This radial drift of banana orbits eventually creates the equivalent radial current which generates the toroidal torque in NTV theory. The term is

equivalent to the third term of LHS in Eq. (1) from Ref. 6 in combined NTV theory. f_L^1 in MARS-K is written as

$$f_L^1 = -f_\varepsilon^0 \varepsilon_k e^{-i\omega t - in\phi} \sum_{m,l} X_m H_{ml} \lambda_l e^{in\tilde{\phi}(t) + im\langle\dot{\chi}\rangle t + il\omega_b t}, \quad (11)$$

where f_ε^0 is the energy derivative of the thermal particle equilibrium distribution function (Maxwellian). $\tilde{\phi}(t) = \phi(t) - \langle\dot{\phi}\rangle t$, where $\langle\cdot\rangle$ denotes the average over the particle bounce period. m corresponds to the Fourier harmonic number along poloidal angle. X_m and H_{ml}, defined in Ref. 20, are related to the perturbed particle Lagrangian H_L

$$H_L = \frac{1}{\varepsilon_k}[Mv_\parallel^2 \vec{\kappa} \cdot \vec{\xi}_\perp + \mu(\vec{Q}_{L\parallel} + \nabla B \cdot \vec{\xi}_\perp)], \quad (12)$$

where $\vec{\kappa} = (\vec{b} \cdot \nabla)\vec{b}$ is the magnetic curvature and $\mu = Mv_\perp^2/2B$ is the particle magnetic moment.

The factor λ_l represents the mode-particle resonance operator

$$\lambda_l = \frac{n[\omega_{*N} + (\hat{\varepsilon}_k - 3/2)\omega_{*T} + \omega_E] + \omega}{n\omega_d - l\omega_b + n\omega_E + \omega + i\nu_{Dl}\hat{\varepsilon}_k^{-3/2}}, \quad (13)$$

where ω_{*N} and ω_{*T} are the diamagnetic drift frequencies associated with the plasma density and temperature gradients, respectively.

With the anisotropic kinetic pressure tensor, the drift kinetic energy of trapped particles is obtained

$$\delta W_k = \frac{1}{2} \int dx^3 \left[p_\perp \frac{1}{B}(\vec{Q}_{L\parallel} + \nabla B \cdot \vec{\xi}_\perp) + p_\parallel \vec{\kappa} \cdot \vec{\xi}_\perp \right]. \quad (14)$$

Substituting Eqs. (4), (5), and (11)–(13) into (14), the drift kinetic energy contributed by the trapped particles in MARS-K can be further written as

$$\delta W_k = -\frac{\pi}{2} \sum_{\alpha=e,i} \frac{1}{M_\alpha^2} \int d\psi_p d\phi \int d\varepsilon_k d\mu \sum_l \frac{\partial f_0}{\partial \varepsilon} \lambda_l \tau_b |\langle \varepsilon_k H_L e^{-il\omega_b t} \rangle_l|^2. \quad (15)$$

Considering the perturbed equilibrium, $\omega \to 0$, one gets

$$\frac{\partial f_0}{\partial \psi_p} = Ze[\omega_{*N} + (\hat{\varepsilon}_k - 3/2)\omega_{*T} + \omega_E] \frac{\partial f_0}{\partial \varepsilon}. \quad (16)$$

The relation of the resonant operators between λ_l in MARS-K and $\mathcal{R}_l$ in IPEC-PENT is

$$Im(\lambda_l)\frac{\partial f_0}{\partial \varepsilon} = -\frac{n}{Ze\omega_b}\frac{\partial f_0}{\partial \psi_p} \mathcal{R}_l. \quad (17)$$

Substituting Eqs. (12) and (17) into (15) with $\omega = 0$, the equivalence between the imaginary part of δW_k in MARS-K and T_ϕ by combining Eqs. (8)–(10) in IPEC-PENT can be established

$$T_\phi = -2nIm(\delta W_k), \quad (18)$$

which agrees with the conclusion in Ref. 11. It indicates that MARS-K has the capability to perform the computation of

neoclassical toroidal viscosity torque based on Eq. (18). Note that the NTV torque computed by IPEC-PENT can also be converted to δW_k based on Ref. 11.

3. Connected NTV in MARS-Q

MARS-Q is a version of MARS that computes NTV torque based on the connected NTV formula in Hamada coordinate.[9,10,25] In this model, the precession resonance ($l = 0$) of trapped particles and a pitch angle scattering collisional operator are taken into account but no bounce resonance ($l \neq 0$) of trapped particles is included. The form of the torque density used in MARS-Q can be written as

$$T_{NTV} = -\tau_{NTV}^{-1} \langle R^2 \rangle_{\psi_p} \rho_i \omega_\phi, \qquad (19)$$

$$\tau_{NTV}^{-1} = \frac{R_0^2}{\langle R^2 \rangle_{\psi_p}} \sum_{\alpha=i,e} \frac{\sqrt{\epsilon} q^2 \omega_{ti}^2}{2\sqrt{2}\pi^{3/2}} \left| \frac{Z_i}{Z_\alpha} \right| \times \lambda_{1,n} \left(1 - \frac{\omega_{nc,n}}{\omega_\phi} \right), \quad (20)$$

$$\lambda_{l,n} = \frac{1}{2} \int_0^\infty I_{\kappa n}(\hat{\varepsilon}_k)(\hat{\varepsilon}_k - 5/2)^{l-1} \hat{\varepsilon}_k^{5/2} e^{-\hat{\varepsilon}_k} d\hat{\varepsilon}_k, \qquad (21)$$

where R_0 is the plasma major radius at plasma center, ρ_i is the ion mass density, $\omega_\phi = \vec{V} \cdot \nabla \phi$ is the ion flow in toroidal direction, $< \cdot >_{\psi_p}$ denotes the flux surface average, q is the safety factor, and Z_α is the charge number of α species. The ion transit frequency ω_{ti}, and $\omega_{nc,n}$, related to diamagnetic frequencies, are defined in Ref. 25.

The analytic solutions of $I_{\kappa n}$ in $1/\nu$, $\nu - \sqrt{\nu}$ and super-banana plateau (SBP) regimes are defined as $I_{\kappa n,1/\nu}$, $I_{\kappa n,\nu-\sqrt{\nu}}$, and $I_{\kappa n,sbp}$, respectively in Refs. 8 and 25. The following smoothly connected formula of $I_{\kappa n}$ in these regimes is considered when MARS-Q solves the NTV torque:

$$I_{\kappa n,C}(\hat{\varepsilon}_k) = \begin{cases} \dfrac{I_{\kappa n,\nu-\sqrt{\nu}}}{1 + I_{\kappa n,\nu-\sqrt{\nu}}/I_{\kappa n,1/\nu}} & (\hat{\varepsilon}_k < x_{min}), \\[3mm] \dfrac{I_{\kappa n,sp}}{1 + I_{\kappa n,sp}/I_{\kappa n,1/\nu}} & (\hat{\varepsilon}_k \geq x_{min}), \end{cases} \qquad (22)$$

where $x_{min} = |\omega_E/\omega_{B0}|$, ω_{B0} is the magnetic drift of the deeply trapped particles with $\hat{\varepsilon}_k = 1$.

It is known that the electron collisionality ν_e and the bounce frequency of electrons are normally larger than $\mathbf{E} \times \mathbf{B}$ drift frequency and ν_i. Therefore, the NTV torque is usually dominated by the contribution of ions, particularly in the bounce resonance case. However, when the collisionality is low, the NTV torque due to the precession resonance of trapped electrons can also be important.[25] In order to simplify the comparison and show a clear correlation among the three approaches, the following discussion will only focus on the ion contributed NTV torque.

III. NUMERICAL RESULTS

A. Perturbed equilibrium

We consider a simple tokamak equilibrium with a circular cross-section which is stable to the ideal kink mode. The toroidal field at the magnetic axis $R_0 = 2$ m is assumed to be $B_0 = 1.0$ T. The aspect ratio is $R/a = 10$, where a is the minor radius of plasma. The safety factor profile is shown in Figure 1, where $q_0 = 1.1$ and $q_a = 2.52$. The ion and electron density have $n_i = n_e$, the ion density n_{i0} and electron density n_{e0} at plasma center vary from 10^{18} m^{-3} to 10^{21} m^{-3}. The plasma pressure profile $P = n_i T_i + n_e T_e$ is fixed. Therefore, the ion temperature T_i and electron temperature T_e, with $T_i = T_e$, are varied from 6.05 keV to 3×10^{-2} keV correspondingly,
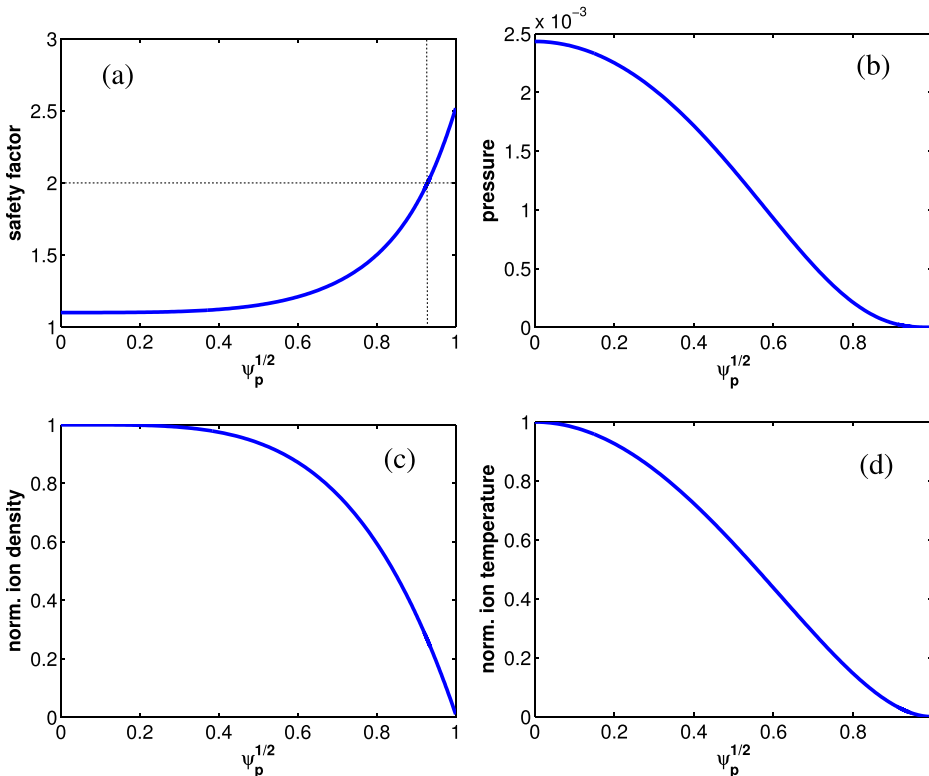

FIG. 1. The safety factor q (a), the equilibrium pressure (b), ion density (c), and ion temperature (d) profiles are plotted as functions of $\psi_p^{1/2}$, where ψ_p is the poloidal flux. The pressure is normalized by B_0^2/μ_0. The plasma density and the temperature profiles are normalized to unity at the magnetic axis.
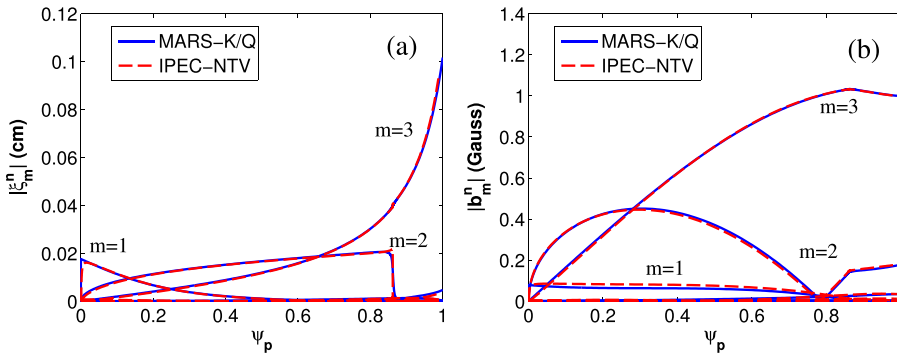
FIG. 2. Comparison of radial profiles of the normal displacement (a) and the normal magnetic perturbation (b) in the presence of an external radial field dominated by $(m,n) = (3,1)$. The poloidal harmonics of plasma response computed by MARS-K/Q (solid lines) and IPEC-PENT (dashed lines) get an excellent quantitative agreement. PEST coordinates are adopted.

where only the thermal particles are considered. IPEC-PENT and MARS-K/Q use this equilibrium to compute the perturbed equilibrium and to numerically verify the equivalence between the NTV torque and the drift kinetic energy. For the sake of simplicity, a uniform profile of $\mathbf{E} \times \mathbf{B}$ drift frequency is considered in this work. Besides the benchmark among the three codes, with this simplified equilibrium, it is also possible to qualitatively investigate the importance of the NTV torque due to precession resonance and the bounce resonance in different collisionality regimes.

In order to compute the NTV torque and the drift kinetic energy, the equilibrium needs to be perturbed by the external field. The same external magnetic perturbations are applied in IPEC-PENT and MARS-K/Q to obtain the perturbed equilibrium. A continuous coil is located close to plasma, $b_c = 1.10a$. By assuming a coil current with a single helical component (3,1), the coil can generate radial magnetic perturbations dominated by the $(m,n) = (3,1)$ harmonic at the plasma edge. Figure 2 shows the perturbed quantities (the normal displacement and the normal magnetic perturbation) computed by MARS-K/Q and IPEC-PENT, respectively. Each poloidal harmonic of the perturbations in the plasma has a very good agreement between IPEC-PENT and MARS-K/Q. This ensures that the three codes are using the same perturbed equilibrium while computing the NTV torque. Since the generated external field is dominated by the (3,1) harmonic having a strength of 1 gauss at the plasma edge where $q_a < 3$, the (3,1) perturbation inside the plasma has the strongest response and penetrates into the plasma without the screening effect. The toroidal coupling enhanced by the finite equilibrium pressure leads to the finite value of other harmonics, e.g., $m = 1$ and $m = 2$ perturbations.

B. Numerical results of NTV torque

1. NTV due to precession resonance of trapped ions

In this section, we first compare the NTV torque contributed solely by the precession motion of trapped ions, based on the perturbed equilibrium described in Sec. III A. In order to better understand the behavior of NTV torque in different collisionality regimes, Figure 3 plots the profiles of magnetic precession frequency ω_d and bounce frequency ω_b of trapped ions which are averaged over the velocity space and the flux surface. Since these profiles and the NTV torque vary along with the poloidal flux ψ_p, we choose the ion thermal frequency at $\psi_p = 0.5$, $\omega_{th} = \sqrt{kT_i/m_i}/R_0$, as the normalization factor, where k is Boltzmann constant. All the

frequencies discussed in this work are normalized by ω_{th}. The averaged ion magnetic precession frequency, $\langle \omega_d \rangle$, is about $0.05\omega_{th}$. Since $\omega_d \sim 1/r$, the magnetic precession frequency increases near the plasma center. The averaged ion bounce frequency, $\langle \omega_b \rangle$, is around $0.25\omega_{th}$. Due to the variation of collisionality and NTV torque along the radial direction, it is difficult to apply the local criterion[8] to estimate the collisionality regime in terms of the global NTV calculation. Therefore, ν^*, ω_E, $\langle \omega_d \rangle$ and $\langle \omega_b \rangle$ are used to estimate the collisionality regimes in this work, where the simplified $\nu^* = \frac{\nu_i(\psi_p=0.5)}{\omega_{th}}$ is chosen as the scan parameter of ion collisionality. In the figures, ν^* at $\psi_p = 0.5$ appears as $\nu^*(\psi_p = 0.5)$ for the convenience of reading.

In Figure 4, two cases, with $\omega_E = 5\omega_{th} \gg \langle \omega_d \rangle$, and $\omega_E = 0.05\omega_{th} \sim \langle \omega_d \rangle$, are chosen to study the collisionality dependence of torque contributed by the precession resonance. In fact, the two cases with high and low ω_E correspond to the non-resonant and resonant cases in Ref. 26, respectively. The ion collisionality profile used in MARS-K (solid), MARS-Q(o), and IPEC-PENT(+) is varied by changing the ion density profile n_i. Meanwhile, the temperature T_i is changed consistently to keep the equilibrium pressure P fixed. Generally, the NTV torque T_ϕ^{MARS-K} computed by MARS-K and T_ϕ^{IPEC} by IPEC-PENT shows a very good quantitative agreement. As for the torque T_ϕ^{MARS-Q} computed
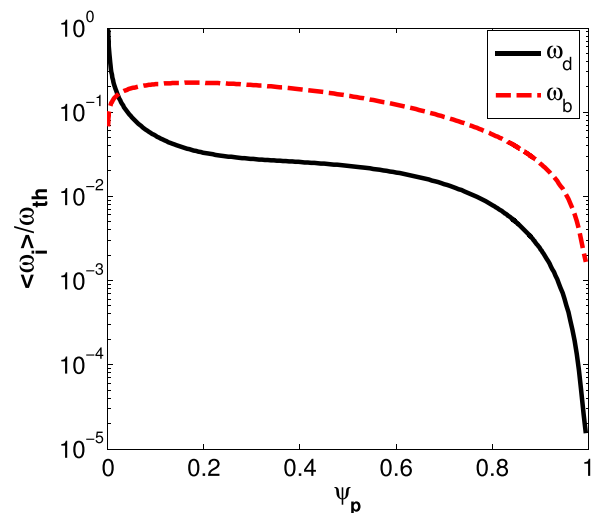

FIG. 3. Radial profiles of magnetic precession frequency (ω_d) and bounce frequency (ω_b) of trapped ions averaged over the velocity space and over the flux surface. The frequencies are normalized by the ion thermal frequency ω_{th} at $\psi_p = 0.5$.
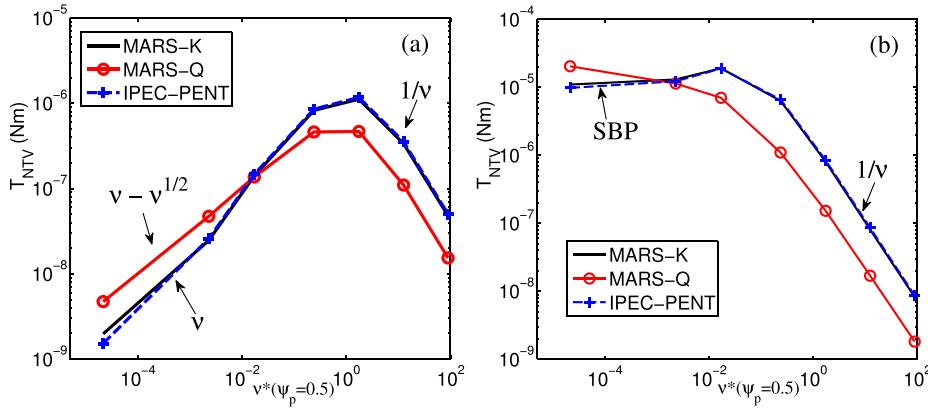
FIG. 4. The comparison of the collisionality ($\nu*$) dependence of NTV torque contributed by the magnetic precession resonance of trapped ions with (a) $\omega_E = 5\omega_{th}$ and (b) $\omega_E = 0.05\omega_{th}$.

by MARS-Q, the tendency of T_ϕ^{MARS-Q} also agrees with T_ϕ^{MARS-K} and T_ϕ^{IPEC} qualitatively.

In Figure 4(a), with the Krook collisional operator, MARS-K and IPEC-PENT can recover the ν regime, when $\nu* < \omega_E/\omega_{th}$ and $\omega_E \gg <\omega_d>$. In the ν regime, the NTV torque, which is proportional to the radial transport, is dominated by particles that undergo detrapping and retrapping processes. The torque scales with ν in this regime. With the same criterion, MARS-Q can further resolve the $\nu - \sqrt{\nu}$, because the connected NTV formula includes the physics of collisional boundary layer by employing the pitch angle scattering operator. Therefore, T_ϕ^{MARS-Q} in the $\nu - \sqrt{\nu}$ regime can be more accurate than the torque computed by the other two codes in the ν regime. When $\nu* > \omega_E/\omega_{th}$, the $1/\nu$ regime is found by the three codes. In this regime, the torque follows the $1/\nu$ scale due to the random walk step size of transport determined by the mean time between collisions. The plateau connecting the ν and $1/\nu$ regimes is also found by the three codes with $\nu* \sim \omega_E/\omega_{th}$. In Figure 4(b), in the SBP regime where $\nu* \ll \omega_E/\omega_{th}$ and $\omega_E \sim <\omega_d>$, ω_E can resonate with the precession frequency of trapped ions and cause the torque. It is noted that T_ϕ^{MARS-K} and T_ϕ^{IPEC} are almost independent of the collisionality which is consistent with the analytical result in Ref. 27. The slight variation of torque is caused by the dependency of torque on n_i and T_i.[8] The torque computed by MARS-Q has more significant variation since the contribution of NTV torque in the $1/\nu$ regime does not vanish due to the smoothly connected NTV formula in Eq. (22). Again, the $1/\nu$ regimes is found by the three codes when $\nu* > \omega_E/\omega_{th}$. Particularly, in this regime, MARS-Q computes a smaller torque than T_ϕ^{MARS-K} and T_ϕ^{IPEC}. While further increasing $\nu_i^* \to \infty$, the factor of 2

difference[26] of the torque due to the difference between the pitch angle scattering operator and Krook collisional operator can be recovered by MARS-Q and IPEC-PENT/MARS-K. The detailed discussion of the collisionality regimes (SBP, ν, $\nu - \sqrt{\nu}$, and $1/\nu$) can be found in Ref. 8.

Figure 5 shows the comparison of the torques computed by MARS-K/Q and IPEC-PENT while scanning $\mathbf{E} \times \mathbf{B}$ rotation frequency ω_E. MARS-K and IPEC-PENT again agree well. The tendency of the torque computed by MARS-Q also agrees with MARS-K and IPEC-PENT results. Figure 5(a) with low collisionality $\nu* = 0.01$ shows that the torque T_ϕ decreases monotonically while the value of ω_E increases. In the high collisionality case, Figure 5(b) indicates that, when $\omega_E \sim 0.1\omega_{th}$ which is much smaller than $\nu* = 50$, the variation of NTV torque T_ϕ becomes less sensitive to the change of ω_E. When ω_E is much larger than $\nu*\omega_{th}$, similar to Figure 5(a), T_ϕ monotonically decreases. These two types of behavior at $\omega_E \gg \nu*\omega_{th}, \omega_d$ and $\nu*\omega_{th} \gg \omega_E, \omega_d$ can be understood by the following simple analysis. In the rotation scan of ω_E, the torque is approximately proportional to the resonant operator $Im(\lambda_l)$ with $\omega = 0$. When $\omega_E \gg \nu*\omega_{th}, \omega_d$, it has $T_\phi \sim \nu_i \hat{\varepsilon}^{-3/2}/\omega_E$ which is monotonically decreased while increasing the value of ω_E. For the case $\nu*\omega_{th} \gg \omega_E, \omega_d$, $T_\phi \sim [\omega_{*N} + (\hat{\varepsilon}_k - 3/2)\omega_{*T}]\hat{\varepsilon}_k^{3/2}/\nu_i$ indicates the torque is independent of $\mathbf{E} \times \mathbf{B}$ drift frequency.

Figure 6 compares the torque density profiles computed by MARS-K, MARS-Q, and IPEC-PENT with $\omega_E = 0.05\omega_{th}$ and $\nu* = 0.01$. It shows that the torque profile computed by MARS-K is very close to IPEC-PENT's result. MARS-Q, which takes into account the different collisionality model and certain geometric simplifications, also presents a similar torque density profile. The above benchmarking results
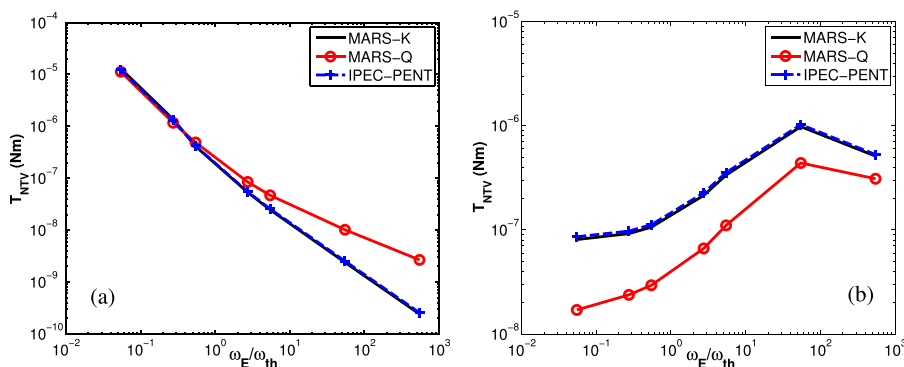

FIG. 5. NTV torque due to the magnetic precession motion of trapped ions is plotted as the function of ω_E. The comparison of torque among MARS-K (solid), MARS-Q ("o") and IPEC-PENT ("+") is made with (a) $\nu* = 0.01$ and (b) $\nu* = 50$.
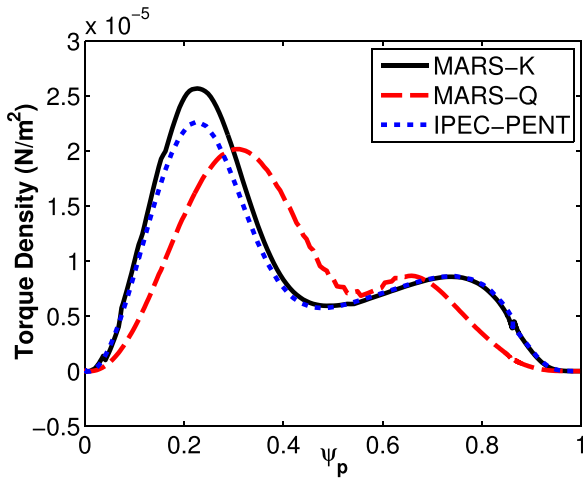
FIG. 6. The torque density profiles computed by MARS-K (solid), MARS-Q (dash), and IPEC-PENT (dot) are compared, where $\omega_E = 0.05\omega_{th}$ and $\nu^* = 0.01$. Only the precession resonance of trapped ions is considered.

FIG. 8. NTV torque is plotted as the function of ω_E with $\nu^* = 0.01$. MARS-K (solid and "o") and IPEC-PENT (dash and "+") computes two cases, respectively: (1) total l case, both precession resonance ($l = 0$) and bounce resonance ($l \neq 0$) are included; (2) $l = 0$ case, only the precession resonance is considered.

present a good validation of all three codes for the NTV computations contributed by the precession resonance of trapped particles.

2. NTV due to bounce motion of trapped ions

Since both the combined NTV theory and the drift kinetic energy can further include the effect of bounce motion of trapped particles (so called bounce resonance ($l \neq 0$) in NTV calculation), these effects in IPEC-PENT and MARS-K are compared in this section. Since the connected NTV formula only includes the precession resonance presently, MARS-Q will not be involved in this bounce resonance study. To better understand the effect of bounce resonance, the conventional regimes of collisionality in terms of precession resonance are still used in the following discussion. Figure 7 compares the computed torque by IPEC-PENT and MARS-K while varying the collisionality ν_i. It shows that the NTV torque computed by the two codes agrees very well while including both precession and bounce resonances (total l case). Moreover, comparing with the precession resonance, it is noted that the bounce resonance can enhance the torque in the ν regime and also slightly increase the torque in the SBP regime. But the torque in the $1/\nu$ regime is dominated by the precession resonance.

The rotation scan of torque with low collisionality $\nu^* = 0.01$ in Figure 8 clearly shows that the bounce
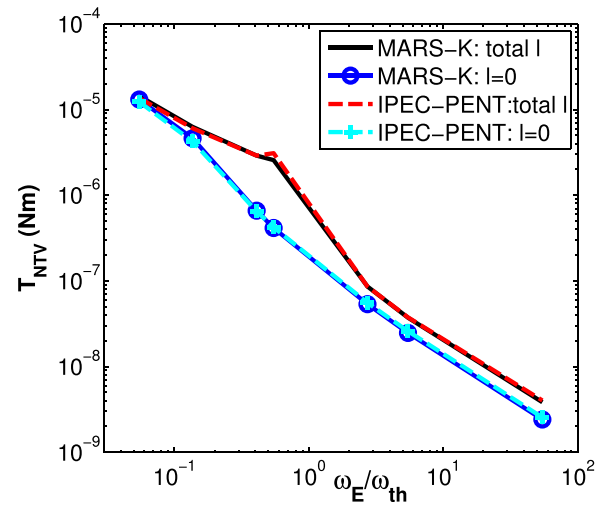
resonance starts to play a major role when the ω_E rotation is comparable with the averaged ion bounce frequency $<\omega_b> \sim 0.25\omega_{th}$, where $E \times B$ drift frequency and the bounce frequency of trapped ions can resonate. When $\omega_E \gg <\omega_b>$, the contribution due to bounce resonance becomes smaller. The torque is mainly contributed by the precession resonance, when $E \times B$ drift frequency is far from the bounce frequency.

In the presence of precession and bounce resonances, Figure 9 also shows a quantitative agreement of torque profiles computed by IPEC-NTV and MARS-K. The different numerical treatment in the two codes causes the slight discrepancy of torque profile near plasma edge but does not affect the agreement between T_ϕ^{MARS-K} and T_ϕ^{IPEC}. In this case with $\omega_E = 0.5\omega_{th}$ and $\nu^* = 0.01$, the bounce resonance has a significant contribution to NTV toque. The torque profile shows that the contribution of bounce resonance is dominant everywhere along the radial direction.

Finally, to clarify in which regime the precession resonance and the bounce resonance can be important, we perform 2D scans of the NTV torque in terms of ω_E/ω_{th} and ν^*. Figure 10(a) presents the distribution of torque only including precession resonance. A large torque due to precession resonance mainly occurs in the SBP regime, the ν
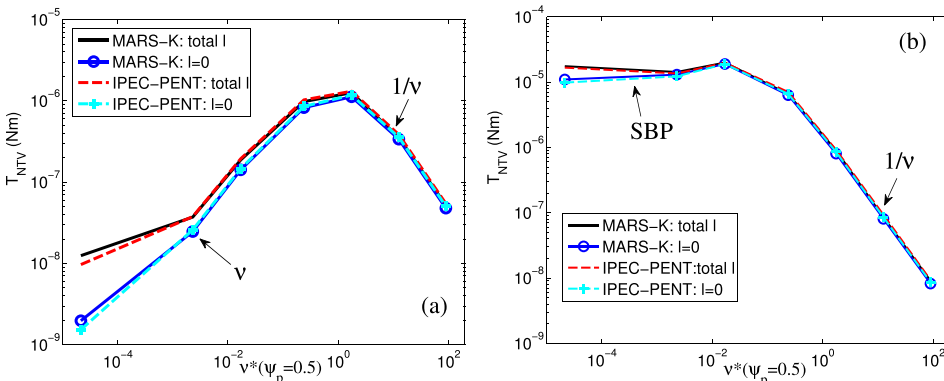

FIG. 7. The collisionality dependence of NTV torque with (a) $\omega_E = 5\omega_{th}$ and (b) $\omega_E = 0.05\omega_{th}$. MARS-K (solid and "o") and IPEC-PENT (dash and "+") computes two cases, respectively: (1) total l case, both precession resonance ($l = 0$) and bounce resonance ($l \neq 0$) are included; (2) $l = 0$ case, only the precession resonance is considered.
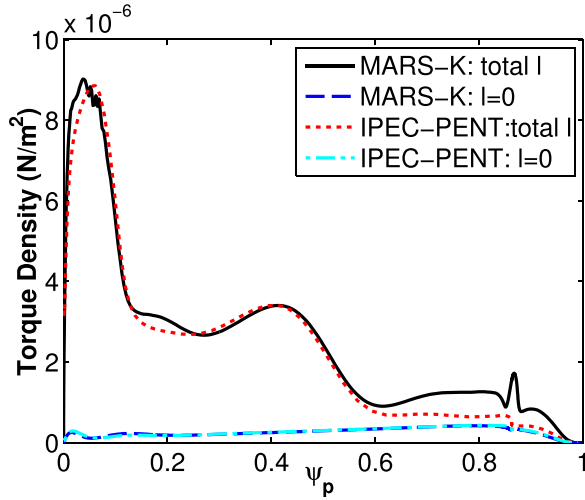
FIG. 9. The torque density profiles computed by MARS-K (solid and dash) and IPEC-PENT (dot and dot-dash) are compared for the total l case and l=0 case denoted in Figure 7, where $\omega_E = 0.5\omega_{th}$ and $\nu^* = 0.01$.

regime with low ω_E/ω_{th} and $1/\nu$ regime with low ν^*. Figure 10(a) shows that the precession resonance contributes a large plateau between ν and $1/\nu$ regimes.

Figure 10(b), only considering the bounce resonance, shows that the bounce resonance can induce a strong torque in similar regimes as the precession resonance except the plateau regime. Particularly, in the ν regime where ω_E can be comparable with $<\omega_b>$, the bounce resonance presents a wider ω_E range having a significant contribution to torque than the precession resonance. In the $1/\nu$ and plateau regime, the bounce resonance induced torque decreases more quickly than the torque contributed by the precession resonance, since the bounce motion of trapped particles can be strongly affected by the collisionality. It is known that, in the regime where the resonance effect is dominant, the details of the collisional operator are not important to NTV torque. Therefore, the Krook collisional operator used by IPEC-PENT and MARS-K can be appropriate in the bounce resonance. However, in the other regimes where collisionality does become important, it requires the further investigation of the NTV torque with Krook model, such as careful comparison of results with the NTV theory developed in Eulerian approach which has the capability to include the complex Coulomb collisional operator.[28]

Figure 11 further shows the relation between the precession resonance and the bounce resonance of trapped ions
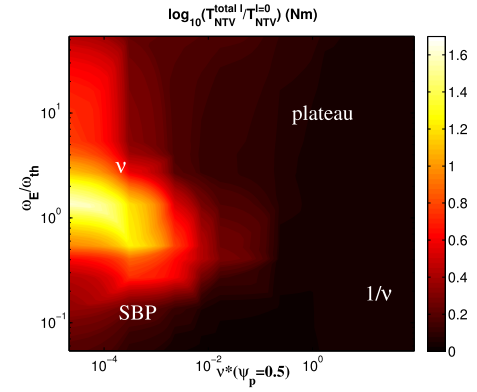

FIG. 11. The ratio of torque $T_{NTV}^{total\,l}/T_{NTV}^{l=0}$ is plotted as the function of ω_E/ω_{th} and ν^*. MARS-K is used to perform the computation. IPEC-PENT agrees with these results.

clearly. The ratio $T_{NTV}^{total\,l}/T_{NTV}^{l=0}$ has the maximum value in the ν region with relatively small ω_E, where $T_{NTV}^{total\,l}$ includes both precession and bounce resonances, and $T_{NTV}^{l=0}$ denotes the torque due to the precession resonance. The maximum value of $T_{NTV}^{total\,l}$ can be about 40 times larger than $T_{NTV}^{l=0}$ in the perturbed equilibrium considered here. It indicates that the bounce resonance can significantly enhance the NTV torque in the ν regime when ω_E enters the range of ion bounce frequencies with low collisionality. Similar results are also observed in particle simulations[29] and in KSTAR experiments.[1] DIII-D experiments also indicate the importance of the bounce resonance in the context of drift kinetic stabilization of resistive wall mode.[30] Because of the equivalence between the NTV torque and the drift kinetic energy, Reimerdes's finding also implies that the bounce resonance enhanced NTV torque can be important in DIII-D plasmas. Furthermore, as for the ITER rotation, the prediction varies in a wide range[31–33] depending on different assumptions. Since Figure 11 indicates that, with a wide range of ω_E, the torque, contributed by the bounce resonance, can be comparable to that by the precession resonance in the low collisionality (SBP and ν) regimes, potentially, the bounce resonance contribution to the torque may not be ignorable in ITER as well.

IV. SUMMARY

In summary, we have shown the equivalence between the drift kinetic energy equation (15) used in MARS-K and the torque expression (8) in the combined NTV theory. This agrees
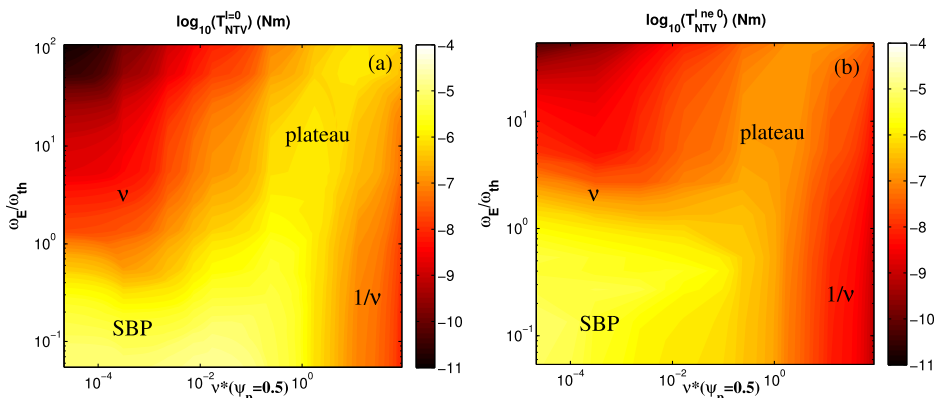

FIG. 10. The ω_E/ω_{th} and ν^* dependence of NTV torque with (a) only precession resonance $T_{NTV}^{l=0}$ and (b) the bounce resonance $T_{NTV}^{l\neq0}$. MARS-K is used to perform the computation. IPEC-PENT agrees with these results.

with $T_\phi = 2in\delta W_k$ as in Ref. 11. A successful numerical benchmarking among three different approaches of NTV theory has been carried out by applying IPEC-PENT, MARS-K, and MARS-Q to the identical equilibrium. In the case of considering the precession resonance ($l = 0$) alone, IPEC-PENT (combined NTV) and MARS-K (equivalence between NTV torque and drift kinetic energy) show an excellent agreement as expected from our analytical derivations. The NTV torque computed by MARS-Q (connected NTV formula) also qualitatively agrees with the results of IPEC-PENT and MARS-K in different collisionality regimes. The difference is mainly due to the geometric simplification and the more complicated collisionality model used in MARS-Q. However, it is important that the tendency of torque computed by the three codes agrees well when we scan the collisionality $\nu*$ and the $\mathbf{E} \times \mathbf{B}$ drift frequency ω_E. The NTV torque further including the bounce resonance ($l \neq 0$) is also compared between IPEC-PENT and MARS-K. Again, IPEC-PENT and MARS-K show a very good agreement. Comparing with the precession resonance case, the rotation ω_E and collisionality $\nu*$ scan indicates that the bounce resonance can significantly enhance the NTV torque in the low collisionality regime ($\sim\nu$ regime) when ω_E reaches the bounce resonance condition. The focus of the present work is on the verification of various NTV theories. For this purpose, we have made simplifications to our plasma model. A simple equilibrium and a uniform $E \times B$ flow have been assumed. The quantitative physics results are of secondary concern in terms of the importance in this work. However, these results are still qualitatively correct, but would require consideration of more realistic plasma models (the specific experimental equilibrium and profiles), in order to be used for quantitative comparison with experiments. As a result of the successful benchmarking, we claim that the computational tools (e.g., IPEC-PENT, MARS-K/Q) are ready to perform quantitative predictions for real devices, although such quantitative and systematic computations remain to be carried out in the future.

We point out that each of the three NTV approaches/codes considered in this work has its own advantages and disadvantages when used for the NTV computations. In particular, IPEC-PENT and MARS-K employ full toroidal geometry and can include both precession and bounce resonances for trapped particles. But so far only the simple Krook collisional operator has been implemented in both codes. On the other hand, the semi-analytic theory that smoothly connects various NTV regimes (as implemented in MARS-Q) includes the pitch angle scattering operator which is probably more capable of describing the particle collisions, in particular, towards the lower collisionality regime (e.g., in the $\nu - \sqrt{\nu}$ regime). The semi-analytic theory has to make certain geometric simplifications. Also the present theory does not treat the particle bounce resonance. In the future, it is desirable to further advance the IPEC-PENT/MARS-K models, to include the pitch angle scattering collision. We also remark that it appears the latter may not always be important for the NTV computations. One recent example is shown in Ref. 1, where the IPEC-PENT results, with only the Krook collision but including the bounce resonances, match well with the measured NTV torque, both amplitude and profile, in KSTAR experiments.

IPEC-PENT and MARS-K both can include the kinetic effect due to passing particles, which may be important when the plasma rotation reaches above the ion acoustic speed. If the NTV torque calculation could be treated appropriately for passing particles, IPEC-PENT and MARS-K would be applied to investigate this effect. In a future study, the possibility of including the passing particle induced NTV torque will be investigated. NTV calculation is usually based on the perturbed equilibrium calculated by the fluid MHD equation (the perturbative approach). MARS-K can also include kinetic pressures $p_\parallel$ and $p_\perp$ into MHD equations self-consistently to study the MHD instability.[16,20] Since we have demonstrated that MARS-K has the capability to perform both perturbed equilibrium and NTV torque computations, it is possible to use MAR-K to solve the perturbed equilibrium and NTV torque in a non-perturbative approach. This capability can help us to understand the interaction between the NTV torque and the plasma response particularly when β is high.[34,35] This subject will be studied in the future work. Moreover, the NTV torque can also be derived in the Eulerian approach. The approach formulates the torque by considering both trapped and passing particles. Particularly, the Eulerian approach also use the Krook collisional operator for the bounce resonance and the transit resonance since the torque is not sensitive to the details of the collisional operator when these resonances are dominant effects.[28] Therefore, it will be necessary to compare this approach with IPEC-PENT and MARS-K/Q, in particular, when the connected NTV formula is developed to include the bounce resonance and transit resonance. It is important to carry out the comprehensive comparison of the NTV theory and the more complete cross-benchmarking to understand the relation among different approaches in the future, where the particle simulation approach should also be involved.

ACKNOWLEDGMENTS

[1] J.-K. Park, Y. M. Jeon, J. E. Menard, W. H. Ko, S. G. Lee, Y. S. Bae, M. Joung, K.-I. You, K.-D. Lee, N. Logan, K. Kim, J. S. Ko, S. W. Yoon, S. H. Hahn, J. H. Kim, W. C. Kim, Y.-K. Oh, and J.-G. Kwak, Phys. Rev. Lett. **111**, 095002 (2013).
[2] Y. Sun, Y. Liang, H. R. Koslowski, S. Jachmich, A. Alfier, O. Asunta, G. Corrigan, C. Giroud, M. P. Gryaznevich, D. Harting, T. Hender, E. Nardon, V. Naulin, V. Parail, T. Tala, C. Wiegmann, S. Wiesen, and JET-EFDA contributors, Plasma Phys. Controlled Fusion **52**, 105007 (2010).
[3] A. M. Garofalo, K. H. Burrell, J. C. DeBoo, J. S. deGrassie, G. L. Jackson, M. Lanctot, H. Reimerdes, M. J. Schaffer, W. M. Solomon, and E. J. Strait, Phys. Rev. Lett. **101**, 195005 (2008).

[4]W. Zhu, S. A. Sabbagh, R. E. Bell, J. M. Bialek, M. G. Bell, B. P. LeBlanc, S. M. Kaye, F. M. Levinton, J. E. Menard, K. C. Shaing, A. C. Sontag, and H. Yuh, Phys. Rev. Lett. **96**, 225002 (2006).

[5]J.-K. Park, A. H. Boozer, J. E. Menard, A. M. Garofalo, M. J. Schaffer, R. J. Hawryluk, S. M. Kaye, S. P. Gerhardt, S. A. Sabbagh, and NSTX Team, Phys. Plasmas **16**, 056115 (2009).

[6]J.-K. Park, A. H. Boozer, and J. E. Menard, Phys. Rev. Lett. **102**, 065002 (2009).

[7]N. C. Logan, J.-K. Park, K. Kim, Z. R. Wang, and J. Berkery, Phys. Plasmas **20**, 122507 (2013).

[8]K. C. Shaing, S. A. Sabbagh, and M. S. Chu, Nucl. Fusion **50**, 025022 (2010).

[9]Y. Q. Liu, A. Kirk, and Y. Sun, Phys. Plasmas **20**, 042503 (2013).

[10]Y. Q. Liu and Y. W. Sun, Phys. Plasmas **20**, 022505 (2013).

[11]J.-K. Park, Phys. Plasmas **18**, 110702 (2011).

[12]M. S. Chu and M. Okabayashi, Plasma Phys. Controlled Fusion **52**, 123001 (2010).

[13]B. Hu and R. Betti, Phys. Rev. Lett. **93**, 105002 (2004).

[14]B. Hu, R. Betti, and J. Manickam, Phys. Plasmas **12**, 057301 (2005).

[15]Y. Q. Liu, M. S. Chu, C. G. Gimblett, and R. J. Hastie, Phys. Plasmas **15**, 092505 (2008).

[16]Z. R. Wang, S. C. Guo, and Y. Q. Liu, Phys. Plasmas **19**, 072518 (2012).

[17]Z. R. Wang, S. C. Guo, Y. Q. Liu, and M. S. Chu, Nucl. Fusion **52**, 063001 (2012).

[18]J. W. Berkery, S. A. Sabbagh, R. Betti, B. Hu, R. E. Bell, S. P. Gerhardt, J. Manickam, and K. Tritz, Phys. Rev. Lett. **104**, 035003 (2010).

[19]J. W. Berkery, S. A. Sabbagh, R. Betti, R. E. Bell, S. P. Gerhardt, B. P. LeBlanc, and H. Yuh, Phys. Rev. Lett. **106**, 075004 (2011).

[20]Y. Q. Liu, M. S. Chu, I. T. Chapman, and T. C. Hender, Phys. Plasmas **15**, 112503 (2008).

[21]J.-K. Park, A. H. Boozer, and A. H. Glasser, Phys. Plasmas **14**, 052110 (2007).

[22]Y. Q. Liu, A. Kirk, and E. Nardon, Phys. Plasmas **17**, 122502 (2010).

[23]J. Wesson, *Tokamaks* (Oxford University Press, New York, 1997).

[24]F. Porcelli, R. Stankiewicz, W. Kerner, and H. L. Berk, Phys. Plasmas **1**, 470 (1994).

[25]Y. Sun, Y. Liang, K. C. Shaing, H. R. Koslowski, C. Wiegmann, and T. Zhang, Nucl. Fusion **51**, 053015 (2011).

[26]Y. Sun, Y. Liang, K. C. Shaing, H. R. Koslowski, C. Wiegmann, and T. Zhang, Phys. Rev. Lett. **105**, 145002 (2010).

[27]K. C. Shaing, S. A. Sabbagh, and M. S. Chu, Plasma Phys. Controlled Fusion **51**, 035009 (2009).

[28]K. C. Shaing, M. S. Chu, and S. A. Sabbagh, Plasma Phys. Controlled Fusion **51**, 075015 (2009).

[29]K. Kim, J.-K. Park, and A. H. Boozer, Phys. Rev. Lett. **110**, 185004 (2013).

[30]H. Reimerdes, J. W. Berkery, M. J. Lanctot, A. M. Garofalo, J. M. Hanson, Y. In, M. Okabayashi, S. A. Sabbagh, and E. J. Strait, Phys. Rev. Lett. **106**, 215002 (2011).

[31]G. M. Staebler and H. E. St John, Nucl. Fusion **46**, L6–L8 (2006).

[32]A. R. Polevoi, S. Yu. Medvedev, V. D. Pustovitov, V. S. Mukhovatov, M. Shimada, A. A. Ivanov, Yu. Yu. Poshekhonov, and M. S. Chu, "Possibility of $Q > 5$ stable, steady-state operation in ITER with moderate β_N and H-factor," in *Proceeding of 19th International Conference on Fusion Energy*, Lyon, France (2002), Paper No. CT/P-08.

[33]R. V. Budny, Nucl. Fusion **49**, 085008 (2009).

[34]A. H. Bozzer, Phys. Rev. Lett. **86**, 5059–5061 (2001).

[35]J.-K. Park, A. H. Boozer, J. E. Menard, S. P. Gerhardt, and S. A. Sabbagh, Phys. Plasmas **16**, 082512 (2009).